This paper is published as part of a PCCP Themed Issue on:
Physical Chemistry of Aerosols

Guest Editors: Ruth Signorell and Allan Bertram (University of British Columbia)

Editorial

Physical Chemistry of Aerosols
Phys. Chem. Chem. Phys., 2009, **DOI:** 10.1039/b916865f

Perspective

Reactions at surfaces in the atmosphere: integration of experiments and theory as necessary (but not necessarily sufficient) for predicting the physical chemistry of aerosols
Barbara J. Finlayson-Pitts, *Phys. Chem. Chem. Phys.*, 2009, **DOI:** 10.1039/b906540g

Papers

Water uptake of clay and desert dust aerosol particles at sub- and supersaturated water vapor conditions
Hanna Herich, Torsten Tritscher, Aldona Wiacek, Martin Gysel, Ernest Weingartner, Ulrike Lohmann, Urs Baltensperger and Daniel J. Cziczo, *Phys. Chem. Chem. Phys.*, 2009, **DOI:** 10.1039/b901585j

Secondary organic aerosol formation from multiphase oxidation of limonene by ozone: mechanistic constraints *via* two-dimensional heteronuclear NMR spectroscopy
Christina S. Maksymiuk, Chakicherla Gayahtri, Roberto R. Gil and Neil M. Donahue, *Phys. Chem. Chem. Phys.*, 2009, **DOI:** 10.1039/b820005j

DRIFTS studies on the photodegradation of tannic acid as a model for HULIS in atmospheric aerosols
Scott Cowen and Hind A. Al-Abadleh, *Phys. Chem. Chem. Phys.*, 2009, **DOI:** 10.1039/b905236d

Infrared spectroscopy of ozone and hydrogen chloride aerosols
Chris Medcraft, Evan G. Robertson, Chris D. Thompson, Sigurd Bauerecker and Don McNaughton, *Phys. Chem. Chem. Phys.*, 2009, **DOI:** 10.1039/b905424n

IR spectroscopy of physical and chemical transformations in cold hydrogen chloride and ammonia aerosols
Evan G. Robertson, Chris Medcraft, Ljiljana Puskar, Rudolf Tuckermann, Chris D. Thompson, Sigurd Bauerecker and Don McNaughton, *Phys. Chem. Chem. Phys.*, 2009, **DOI:** 10.1039/b905425c

Formation of naproxen–polylactic acid nanoparticles from supercritical solutions and their characterization in the aerosol phase
Moritz Gadermann, Simran Kular, Ali H. Al-Marzouqi and Ruth Signorell, *Phys. Chem. Chem. Phys.*, 2009, **DOI:** 10.1039/b901744e

Measurements and simulations of the near-surface composition of evaporating ethanol–water droplets
Christopher J. Homer, Xingmao Jiang, Timothy L. Ward, C. Jeffrey Brinker and Jonathan P. Reid, *Phys. Chem. Chem. Phys.*, 2009, **DOI:** 10.1039/b904070f

Effects of dicarboxylic acid coating on the optical properties of soot
Huaxin Xue, Alexei F. Khalizov, Lin Wang, Jun Zheng and Renyi Zhang, *Phys. Chem. Chem. Phys.*, 2009, **DOI:** 10.1039/b904129j

Spectroscopic evidence for cyclical aggregation and coalescence of molecular aerosol particles
J. P. Devlin, C. A. Yinnon and V. Buch, *Phys. Chem. Chem. Phys.*, 2009, **DOI:** 10.1039/b905018n

Photoenhanced ozone loss on solid pyrene films
Sarah A. Styler, Marcello Brigante, Barbara D'Anna, Christian George and D. J. Donaldson, *Phys. Chem. Chem. Phys.*, 2009, **DOI:** 10.1039/b904180j

Quantifying the reactive uptake of OH by organic aerosols in a continuous flow stirred tank reactor
Dung L. Che, Jared D. Smith, Stephen R. Leone, Musahid Ahmed and Kevin R. Wilson, *Phys. Chem. Chem. Phys.*, 2009, **DOI:** 10.1039/b904418c

Laboratory study of the interaction of HO_2 radicals with the NaCl, NaBr, $MgCl_2 \cdot 6H_2O$ and sea salt surfaces
Ekaterina Loukhovitskaya, Yuri Bedjanian, Igor Morozov and Georges Le Bras, *Phys. Chem. Chem. Phys.*, 2009, **DOI:** 10.1039/b906300e

Kinetics of the heterogeneous reaction of nitric acid with mineral dust particles: an aerosol flowtube study
A. Vlasenko, T. Huthwelker, H. W. Gäggeler and M. Ammann, *Phys. Chem. Chem. Phys.*, 2009, **DOI:** 10.1039/b904290n

Timescale for hygroscopic conversion of calcite mineral particles through heterogeneous reaction with nitric acid
Ryan C. Sullivan, Meagan J. K. Moore, Markus D. Petters, Sonia M. Kreidenweis, Greg C. Roberts and Kimberly A. Prather, *Phys. Chem. Chem. Phys.*, 2009, **DOI:** 10.1039/b904217b

Mid-infrared complex refractive indices for oleic acid and optical properties of model oleic acid/water aerosols
Shannon M. McGinty, Marta K. Kapala and Richard F. Niedziela, *Phys. Chem. Chem. Phys.*, 2009, **DOI:** 10.1039/b905371a

A study of oleic acid and 2,4-DHB acid aerosols using an IR-VUV-ITMS: insights into the strengths and weaknesses of the technique
Sarah J. Hanna, Pedro Campuzano-Jost, Emily A. Simpson, Itamar Burak, Michael W. Blades, John W. Hepburn and Allan K. Bertram, *Phys. Chem. Chem. Phys.*, 2009, **DOI:** 10.1039/b904748d

Deliquescence behaviour and crystallisation of ternary ammonium sulfate/dicarboxylic acid/water aerosols
L. Treuel, S. Pederzani and R. Zellner, *Phys. Chem. Chem. Phys.*, 2009, **DOI:** 10.1039/b905007h

Laboratory chamber studies on the formation of organosulfates from reactive uptake of monoterpene oxides
Yoshiteru Iinuma, Olaf Böge, Ariane Kahnt and Hartmut Herrmann, *Phys. Chem. Chem. Phys.*, 2009, **DOI:** 10.1039/b904025k

Measurement of fragmentation and functionalization pathways in the heterogeneous oxidation of oxidized organic aerosol
Jesse H. Kroll, Jared D. Smith, Dung L. Che, Sean H. Kessler, Douglas R. Worsnop and Kevin R. Wilson, *Phys. Chem. Chem. Phys.*, 2009, **DOI:** 10.1039/b905289e

Using optical landscapes to control, direct and isolate aerosol particles
Jon B. Wills, Jason R. Butler, John Palmer and Jonathan P. Reid, *Phys. Chem. Chem. Phys.*, 2009, **DOI:** 10.1039/b908270k

Reactivity of oleic acid in organic particles: changes in oxidant uptake and reaction stoichiometry with particle oxidation
Amy M. Sage, Emily A. Weitkamp, Allen L. Robinson and Neil M. Donahue, *Phys. Chem. Chem. Phys.*, 2009, **DOI:** 10.1039/b904285g

Surface tension of mixed inorganic and dicarboxylic acid aqueous solutions at 298.15 K and their importance for cloud activation predictions
Alastair Murray Booth, David Owen Topping, Gordon McFiggans and Carl John Percival, *Phys. Chem. Chem. Phys.*, 2009, **DOI:** 10.1039/b906849j

Kinetics of the heterogeneous conversion of 1,4-hydroxycarbonyls to cyclic hemiacetals and dihydrofurans on organic aerosol particles
Yong Bin Lim and Paul J. Ziemann, *Phys. Chem. Chem. Phys.*, 2009, **DOI:** 10.1039/b904333k

Time-resolved molecular characterization of limonene/ozone aerosol using high-resolution electrospray ionization mass spectrometry
Adam P. Bateman, Sergey A. Nizkorodov, Julia Laskin and Alexander Laskin, *Phys. Chem. Chem. Phys.*, 2009, **DOI:** 10.1039/b905288g

Cloud condensation nuclei and ice nucleation activity of hydrophobic and hydrophilic soot particles
Kirsten A. Koehler, Paul J. DeMott, Sonia M. Kreidenweis, Olga B. Popovicheva, Markus D. Petters, Christian M. Carrico, Elena D. Kireeva, Tatiana D. Khokhlova and Natalia K. Shonija, *Phys. Chem. Chem. Phys.*, 2009, **DOI:** 10.1039/b905334b

Effective broadband refractive index retrieval by a white light optical particle counter
J. Michel Flores, Miri Trainic, Stephan Borrmann and Yinon Rudich, *Phys. Chem. Chem. Phys.*, 2009, **DOI:** 10.1039/b905292e

Influence of gas-to-particle partitioning on the hygroscopic and droplet activation behaviour of α-pinene secondary organic aerosol
Zsófia Jurányi, Martin Gysel, Jonathan Duplissy, Ernest Weingartner, Torsten Tritscher, Josef Dommen, Silvia Henning, Markus Ziese, Alexej Kiselev, Frank Stratmann, Ingrid George and Urs Baltensperger, *Phys. Chem. Chem. Phys.*, 2009, **DOI:** 10.1039/b904162a

Reactive uptake studies of NO_3 and N_2O_5 on alkenoic acid, alkanoate, and polyalcohol substrates to probe nighttime aerosol chemistry
Simone Gross, Richard Iannone, Song Xiao and Allan K. Bertram, *Phys. Chem. Chem. Phys.*, 2009, **DOI:** 10.1039/b904741g

Organic nitrate formation in the radical-initiated oxidation of model aerosol particles in the presence of NO_x
Lindsay H. Renbaum and Geoffrey D. Smith, *Phys. Chem. Chem. Phys.*, 2009, **DOI:** 10.1039/b909239k

Dynamics and mass accommodation of HCl molecules on sulfuric acid–water surfaces
P. Behr, U. Scharfenort, K. Ataya and R. Zellner, *Phys. Chem. Chem. Phys.*, 2009, **DOI:** 10.1039/b904629a

Structural stability of electrosprayed proteins: temperature and hydration effects
Erik G. Marklund, Daniel S. D. Larsson, David van der Spoel, Alexandra Patriksson and Carl Caleman, *Phys. Chem. Chem. Phys.*, 2009, **DOI:** 10.1039/b903846a

Tandem ion mobility-mass spectrometry (IMS-MS) study of ion evaporation from ionic liquid-acetonitrile nanodrops
Christopher J. Hogan Jr and Juan Fernández de la Mora, *Phys. Chem. Chem. Phys.*, 2009, **DOI:** 10.1039/b904022f

Homogeneous ice freezing temperatures and ice nucleation rates of aqueous ammonium sulfate and aqueous levoglucosan particles for relevant atmospheric conditions
Daniel Alexander Knopf and Miguel David Lopez, *Phys. Chem. Chem. Phys.*, 2009, **DOI:** 10.1039/b903750k

Dynamics and mass accommodation of HCl molecules on sulfuric acid–water surfaces

P. Behr, U. Scharfenort, K. Ataya and R. Zellner*

Received 6th March 2009, Accepted 21st July 2009
First published as an Advance Article on the web 13th August 2009
DOI: 10.1039/b904629a

A molecular beam technique has been used to study the dynamics and mass accommodation of HCl molecules in collision with sulfuric acid–water surfaces. The experiments were performed by directing a nearly mono-energetic beam of HCl molecules onto a continuously renewed liquid film of 54–76 wt% sulfuric acid at temperatures between 213 K and 243 K. Deuterated sulfuric acid was used to separate sticking but non-reactive collisions from those that involved penetration through the phase boundary followed by dissociation and recombination with D^+. The results indicate that the mass accommodation of HCl on sulfuric acid–water surfaces decreases sharply with increasing acidity over the concentration range 54–76 wt%. Using the capillary wave theory of mass accommodation this effect is explained by a change of the surface dynamics. Regarding the temperature dependence it is found that the mass accommodation of HCl increases with increasing temperature and is limited by the bulk phase viscosity and driven by the restoring forces of the surface tension. These findings imply that under atmospheric conditions the uptake of HCl from the gas phase depends crucially on the bulk phase parameters of the sulfuric acid aerosol.

1. Introductions

Heterogeneous interactions between gas-phase molecules and liquid surfaces are important steps in a wide range of atmospheric and industrial processes. The experimental and theoretical work performed on such processes over the last two decades was motivated to a great extent by their importance in the atmosphere, where gas–liquid interactions are key steps in acid deposition, stratospheric ozone depletion, cloud processing and aerosol-induced haze (see *e.g.* Finlayson-Pitts and Pitts, 2000;[1] Zellner, 1999[2]). Even though the amount of condensed phase material in the atmosphere is generally small, the collision rate of gaseous pollutants with atmospheric particles can be relatively high and easily be competitive with pure gas phase chemistry.

The collision of a gas molecule with a liquid/solid surface may be regarded as the first step of a heterogeneous interaction. The possible results of such collisions include the incorporation of the species into the condensed phase, the formation of a surface complex as well as reaction at the surface or in the bulk. Depending on its solubility, the product molecule from such reactions may return into the gas phase or remain in the condensed phase. Jointly, the detailed pathways and kinetics of such transformations determine their importance in atmospheric processes.[3–5] Under stratospheric conditions the heterogeneous interaction and solubility of HCl in sulfuric acid aerosols is a critical parameter in determining the effectiveness of the halogen activation reactions from the halogen reservoir species such as $ClONO_2$ or HOCl (*e.g.* ref. 2). A schematic summary of the various processes that represent the overall uptake of HCl on H_2SO_4–water solutions is shown in Fig. 1.

The kinematic details of the initial impact of a molecule colliding with a surface determines whether it scatters away from the surface (inelastic scattering) or dissipates its excess energy through one or several bounces and finally binds to interfacial H_2O or H_2SO_4 (thermalization and sticking (S)). Molecules that become trapped at the interface may desorb and return back into the gas phase by the thermal motions of the surface atoms (k_{des}). Alternatively, if HCl molecules form strong hydrogen bonds to surface OH or SO groups, they may become sufficiently solvated (k_{sol}) to dissociate into H^+ and X^- in the interfacial region.

In the case of a non-reactive interaction with the condensed phase, the overall flux of the gas into the liquid is determined by the transport from the gas phase to the surface, the relative rates of adsorption and desorption at the surface, and the rates

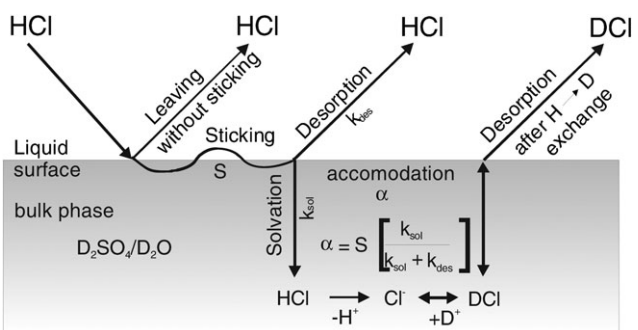

Fig. 1 Schematic representation of possible interactions of gas phase HCl molecules with a liquid sulfuric acid–water surface, showing non-reactive and reactive processes.

Institute of Physical Chemistry, University of Duisburg-Essen, D-45117 Essen

of transfer into the bulk of the liquid as well as back to the surface. In general, the time dependent concentration change in the gas and condensed phase may be described by a set of coupled differential equations, for which analytical solutions exist only for a few limited cases.[6] The so-called resistor model, which uses steady-state solutions that decouple the differential equations for each process, has been shown to provide a good approximation to the numerical solutions.[7,8] In this model each process is formulated in terms of a resistance which is the inverse of an uptake coefficient (γ), *viz.*

$$\frac{1}{\gamma} = \frac{1}{\Gamma_{\mathrm{diff}}} + \frac{1}{\alpha} + \frac{1}{\Gamma_{\mathrm{sat}}} \quad (1)$$

In here, Γ_{diff} is the limiting factor for diffusion in the gas phase towards the liquid surface, whereas the mass accommodation, α, is given by:

$$\frac{1}{\alpha} = \frac{1}{S} + \frac{k_{\mathrm{des}}}{S k_{\mathrm{sol}}} \quad (2)$$

where S is the sticking coefficient and k_{des} and k_{sol} are the first-order rate coefficients for desorption and solvation, respectively. In uptake measurements the sticking coefficient is assumed to be typically close to unity for gas–liquid collisions occurring near room temperature with thermal speeds.[9,10] It should be noted, however, that velocity resolved molecular beam experiments on liquid surfaces which allow a direct determination of S, indicate that this parameter depends on the mass, the approaching angle and the translational energy of the impinging gas as well as on bulk phase parameters and the temperature of the liquid phase.[11] The resistance due to solubility limitation (liquid-phase saturation) of eqn (1) is given by[8,12]

$$\frac{1}{\Gamma_{\mathrm{sat}}} = \frac{c}{4HRT}\sqrt{\frac{t\pi}{D_{\mathrm{l}}}} \quad (3)$$

where R (atm l mol^{-1} K^{-1}) is the gas constant, T/K is the gas-phase temperature, H (M atm^{-1}) is Henry's law coefficient describing the solubility of the gas-phase species in the liquid, t (s) is the gas–liquid interaction time, and D_{l} (cm^2 s^{-1}) is the liquid-phase diffusion coefficient for the dissolving species.

Motivated by the role of sulfuric acid particles in heterogeneous reactions in the atmosphere[13] the uptake kinetics and dynamics of gaseous HCl in contact with liquid sulfuric acid solutions have been studied using different experimental techniques including Knudsen cells,[14,15] coated flow tubes,[8,16] droplet trains[17,18] molecular beams[19,20] and single levitated micro-droplets.[21–23] Independent of the experimental technique applied, all observations indicate that the uptake of gaseous HCl into aqueous sulfuric acid depends strongly on the H_2SO_4 concentration. With the H_2SO_4 concentration increasing towards its normal stratospheric value of 60–80 wt% the observed uptake coefficients of HCl decrease.[24,25]

Despite the consistency of these observations the individual processes (mass accommodation (α), solubility (H), or bulk phase diffusion (D_{liq}), which can each independently limit the uptake into the condensed phase, are differently evaluated. Time dependent uptake measurements as performed by *i.e.* Knudsen cells or droplet trains led to an expression for $\sqrt{(\mathrm{HD})}$ which shows a decrease in the solubility with increasing acidity. Between 50–60 wt% the reported (HD) values of Robinson *et al.*[18] are in reasonable agreement with values of H and D as derived by Carslaw *et al.*[26] and Klassen *et al.*[27] whilst experimental and theoretical (HD) values at 70 wt% differ by almost an order of magnitude. It is interesting to note though that the mass accommodation coefficient, α, has been identified to be almost unity, independent of the composition of the sulfuric acid–water solution (Robinson *et al.*[18]). Detailed dynamical studies of HCl interacting with D_2SO_4 at 213 K, as performed by Behr *et al.*,[19] on the other hand indicate that the mass accommodation coefficient α decreases strongly from 0.72 to 0.11 as the acid concentration increases from 52.5 to 70.5 wt%.

Using single levitated micro-droplets to perform measurements of the uptake dynamics and diffusion of HCl in sulfuric acid solutions, Schwell *et al.*[21] reported that at low temperatures and intermediate sulfuric acid concentrations ($T < 190$ K for 48 wt% H_2SO_4 and $T < 195$ K for 56 wt% H_2SO_4, respectively) liquid-phase diffusion in the droplet is the rate-limiting step in the overall uptake process. At higher temperatures and lower sulfuric acid concentrations (30–40 wt% H_2SO_4, T = 185–207 K), on the other hand, gas-phase diffusion followed by subsequent accommodation/dissolution at the liquid surface is rate controlling. These results, however, are in contrast to other information available in the literature.[18,19] The reported value[21] of $\alpha \sim 10^{-2}$ is two orders of magnitude lower than that published for the same temperature and concentration range elsewhere in the literature.[18]

In order to model chemical processes in stratospheric particles a more exact knowledge of the rate limiting steps is necessary.[28] This applies in particular to conditions with incomplete chlorine activation on the mesoscale (see *e.g.* Carslaw *et al.*[29]). However, as discussed above, crucial parameters such as the liquid phase diffusion coefficient and the accommodation coefficients are evaluated differently in the literature. In addition, these parameters are difficult to measure with standard laboratory approaches at stratospheric temperatures.[8,14,15,18,27,30,31]

In principle, molecular beam experiments on liquid surfaces provide an experimental technique to investigate the dynamics and kinetics of heterogeneous interactions on fluid interfaces and to distinguish between the different elementary processes. In the present work deuterated sulfuric acid–water solutions were used to separate non-reactive collisions from those that involved penetration through the phase boundary followed by dissociation and recombination with D^+. In addition we separate and quantify the mass accommodation coefficient in dependence of the acid concentration and the surface temperature.

2. Experimental

The experiments were performed with a molecular beam scattering technique similar to the one developed by Nathanson and coworkers.[32,33] A schematic representation of the experimental set-up is shown in Fig. 2. Since this set-up has recently been described in more detail[11] we will only emphasis its major aspects as relevant to the present work. A continuous

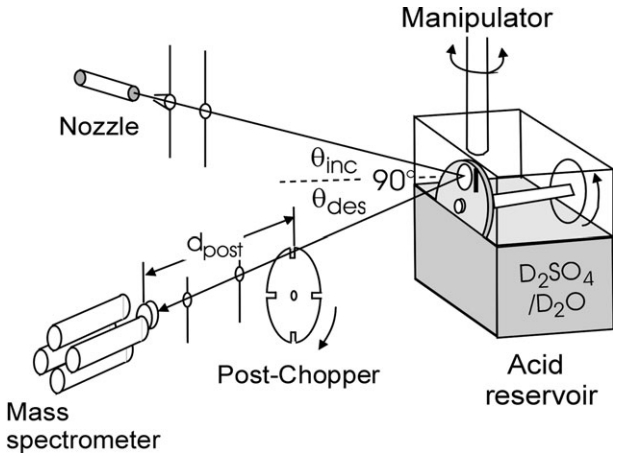

Fig. 2 Schematic representation of experimental set-up.

molecular beam of HCl is created by expanding a gas mixture at 1.0–1.2 bar through an aperture of ~0.1 mm in diameter. Whereas the expansion of pure HCl gas generates initial translational energies of almost (5/2) RT (~6 kJ mol^{-1} at 298 K), hyper-thermal translational energies up to 140 kJ mol^{-1} were achieved by seeding the HCl molecules with H_2 and by varying the nozzle temperature. To reduce the contribution of dimers in the beam our nozzle temperature was raised to values between 80 and 150 °C. The monomer/dimer ratio has been determined from the ratio of the ms peaks at $m/z = 38$ $(H^{37}Cl)^+$ and $m/z = 39$ $(H_2{}^{37}Cl)^+$ and has usually been found to be larger than 20. Continuously renewed liquid films of D_2SO_4–D_2O as a target were generated by partially immersing a vertically rotating wheel in the acid. The reservoir depicted in Fig. 2 shows a 4.5 cm in diameter gold coated brass wheel which is partially submersed in the liquid. The liquid reservoir is suspended from a post which can be rotated in order to vary the incident angle of the molecular beam. The rotation speed of the wheel was varied between 0.025 and 0.25 Hz. The reservoir is filled with 15 ml of a degassed sulfuric acid–water mixture. It is cooled by circulating a cold methanol–ethanol mixture through Teflon coated cooling tubes that pass through the liquid.

The experiments were performed with sulfuric acid concentrations ranging from ~54 to 76 wt% for which the acid is still liquid and the results are not significantly affected by the collisions of the impinging gas with desorbing water molecules.

The molecules that scatter or desorb from the liquid interface are detected by a doubly differentially pumped mass spectrometer with cross beam ionisation (QMG 422, Balzers (Pfeiffer-Vacuum)) oriented at a fixed angle of 90° to the incident beam. This fixed geometry allows scattered signals to be detected only at $\theta_{fin} = 90° - \theta_{inc}$. The flight times of the scattered or desorbing species are determined by chopping the flux of the recoiling atoms into short pulses with a 10 cm in diameter spinning wheel with two 4 mm slots. This method generates 67 μs pulses with the wheel spinning at 200 Hz. The arrival times of the products are then measured at the MS ioniser which is positioned 28.0 ± 0.2 cm away from the chopper. The TOF spectra are recorded by a multichannel scaler (Fast, P7882-2) in 0.25 μs bins. It needs to be emphasised that in the post-chopper configuration the chopper wheel in Fig. 2 is positioned between the surface and the mass spectrometer. Hence we measure velocity distributions of the recoiling molecules and not the residence times of the gas on or in the liquid.

3. Results

In the following we discuss post-chopper measurements of H → D exchange in collisions of HCl with a deuterated sulfuric acid–water surface. The post-chopper spectra observed are plots of the mass spectrometer signal *versus* the flight time for molecules to traverse the distance d_{post} at $\theta_{inc} = \theta_{fin} = 45°$. All spectra are corrected for electronic and timing offsets.[11] The QMS signal is proportional to the number density, $N(t)$, and is used to compute the relative fluxes or probability $P(E_{fin})$, that a molecule will scatter with translational energy E_{fin}. The energy distribution is computed from the relation $P(E_{fin}) \sim N(t)t^2$ and $E_{fin} = 1/2m_{gas}(L/t)^2$, where C is a normalization constant and L is the 28 cm flight path.

Fig. 3a–c show the superposition of TOF-spectra for $H^{37}Cl$ (open squares) and $D^{37}Cl$ molecules (filled squares). The spectra were recorded in collisions of HCl with deuterated sulfuric acid–water solution surfaces of 68 wt% (Fig. 3a,b) and 60 wt% (Fig. 3c), respectively, at 213 K. The detection of the molecules at $m/z = 38$ ($H^{37}Cl$) and $m/z = 39$ ($D^{37}Cl$) ensures that ^{37}Cl atoms from the fragmentation of $H^{37}Cl$ in the mass spectrometer do not contribute to the DCl signal.

The open squares shown in Fig. 3 indicate that HCl molecules at high initial translational energies scatter in a bimodal distribution. The sharper peak at earlier arrival time is composed of molecules recoiling at high velocities. This inelastic or impulsive scattering channel, IS, contains species which scatter from the surface and deposit only a fraction of their kinetic energy into the liquid phase molecules.[19,20,33] The peak at later arrival times, corresponding to low final energies, closely follows a Maxwell–Boltzmann distribution at T_{liq} and is assigned to the trapping–desorption channel, TD. This component is hence attributed to molecules that dissipate their energy fully and thermalize at the surface before desorption. The solid curves in the TOF spectra show the TD components as assigned by the component of $P(E_{fin})$ that corresponds to a Boltzmann distribution,[19,20] *viz.*

$$P_{TD}(E_{fin}) = E_{fin}(RT_{liq})^{-2} \exp(-E_{fin}/RT_{liq}) \quad (4)$$

The IS contribution is assigned to the difference between $P(E_{fin})$ and $P_{TD}(E_{fin})$, constrained such that $P_{IS}(E_{fin}) = 0$ at $E_{fin} = RT_{liq}$.

The TOF distributions for HCl molecules that have undergone H → D exchange to generate DCl is shown by the filled squares in Fig. 3a–c. It is noted that all DCl molecules desorb from the surface with velocities obeying a Maxwell–Boltzmann distribution. This demonstrates that there is no proton exchange process which bypasses the step of thermal equilibration.

The number of molecules desorbing thermally from the acid at $\theta_{fin} = 45°$ is proportional to the integrated thermal

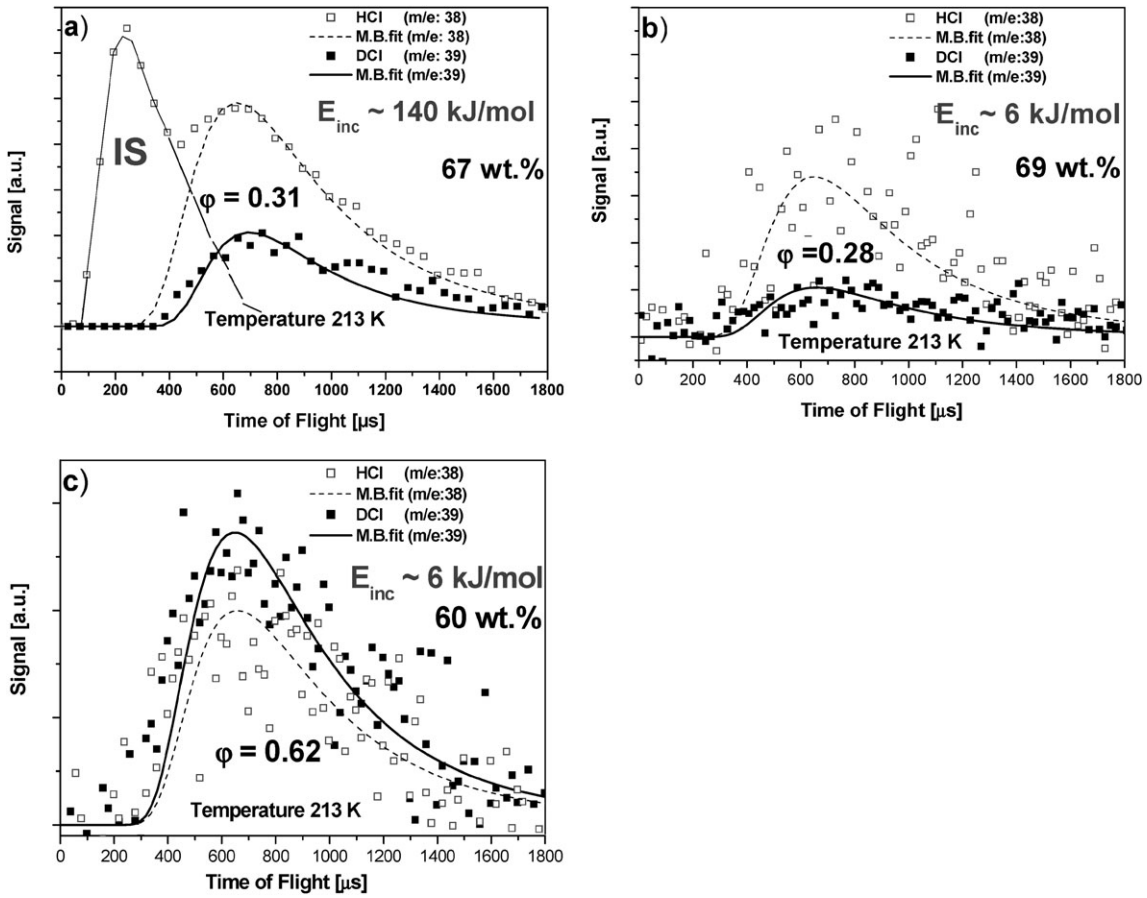

Fig. 3 (a–c) Observed intensity profiles of backscattered HCl-atoms from a sulfuric acid–water surface at $T = 213$ K. (a) TOF spectrum of HCl (open squares) and DCl (filled squares) following collision of $E_{inc} \sim 140$ kJ mol^{-1} HCl with 67 wt% D_2SO_4 at 213 K. The dashed (HCl) and solid (DCl) curves are Maxwell–Boltzmann distribution fits to the TD component. The left hand peak of the HCl signal corresponds to the inelastic scattering (IS) peak. (b,c) TOF spectra of HCl (open squares) and DCl (filled squares) after collision of $E_{inc} \sim 6$ kJ mol^{-1} HCl with 69 wt% (b) and 60 wt% (c).

desorption intensity for HCl (TD_{HCl}) and DCl (TD_{DCl}), respectively, and is equal to:

$$TD_{HCl} + TD_{DCl} = \int P_{TD}{}^{HCl}(E_{fin})\, dE_{fin} + \int P_{TD}{}^{DCl}(E_{fin})\, dE_{fin} \quad (5)$$

Therefore, the fraction of molecules (f_{exch}) that thermally emerges as proton-exchanged DCl is

$$f_{exch} = TD_{DCl}/(TD_{DCl} + TD_{HCl}). \quad (6)$$

Residence time measurements using short pulses of the incident beam permit to correct all f_{exch} values for the small fraction of HCl molecules that remain in the acid after the exposure time of 0.23 s. Futhermore, the total balancing of the HCl–DCl fluxes at $\theta_{fin.} = 45^\circ$ indicates that the angular distributions of the thermally desorbing HCl and DCl are similar and together represent the total flux of desorbing molecules. Uptake measurements, which integrate over all exit angles, support the TOF calculations of f_{exch}.[20]

Fig. 4 summarises the experimental results for the proton exchange fraction, f_{exch}, in dependence of the composition of the liquid film at 213 K. As can be seen, the f_{exch} values decrease significantly with increasing acid concentration, indicating that immediate desorption competes more effectively with dissociation at higher acid concentrations. This trend in f_{exch} also implies that H → D exchange increases with dilution since more D_2O molecules are available for

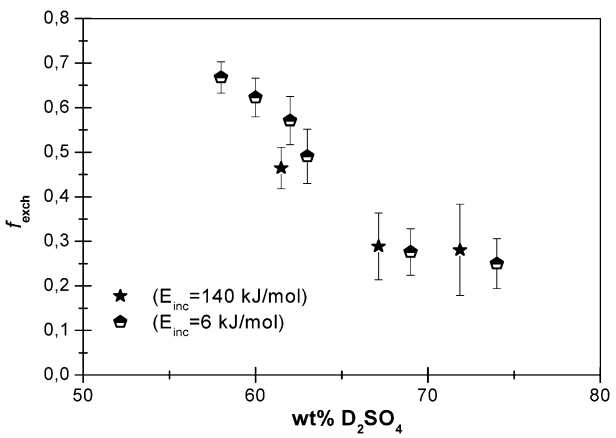

Fig. 4 Summary of experimental results for the proton exchange fraction in dependence of the composition of the liquid phase between 57–74 wt% sulfuric acid at 213 K and different initial energies. Each data point is the average of 3–4 individual measurements. The error bars correspond to the statistical deviations.

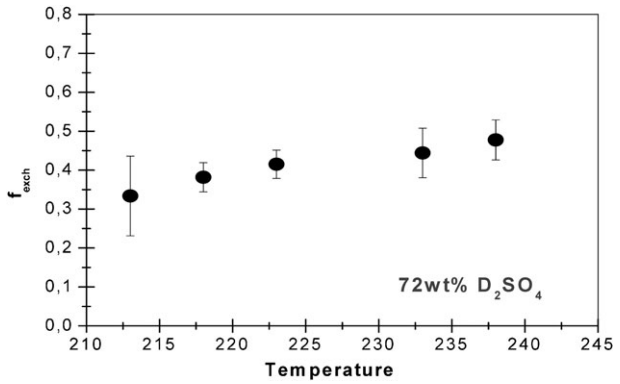

Fig. 5 Summary of experimental results for the proton exchange fraction in dependence of the temperature of the sulfuric acid film between 213 and 238 K and for 72 wt% acidity. Each data point is the average of 5–6 individual measurements. The error bars correspond to the statistical deviations.

hydrogen bonding and protonation. This enables the gas molecule to be captured more effectively during the time between trapping and desorption.

Similar values for f_{exch} were obtained for different incident energies, even though the inelastic scattering contribution diminishes at lower E_{inc}. As discussed later, the thermal desorption of product DCl and the invariance of f_{exch} with E_{inc} imply that only thermalized HCl molecules undergo H → D exchange.

The experimental results for the proton exchange fraction in dependence of the temperature of the sulfuric acid target between 213 and 238 K are shown in Fig. 5.

As can be seen from this Figure the proton exchange fraction measured at 70 wt% sulfuric acid increases from 0.33 at 213 K to 0.47 at 237 K. This trend in f_{exch} implies that proton exchange accelerates with fluctuations in regions near the interface, enabling the gas molecule to be captured more effectively during the time between trapping and desorption.

4. Discussion

4.1 H → D exchange as a function of acid concentration and temperature

As demonstrated in Fig. 3a–c the energy transfer for inelastically scattered HCl molecules on D_2SO_4–H_2O surfaces as well as for their thermalization and desorption is accompanied by the desorption of DCl with velocities obeying a Maxwell–Boltzmann distribution corresponding to the surface temperature.

In agreement with literature data[19,20] our results also reveal that the H → D exchange rate, based on the fraction of thermalized molecules, is independent on the incident energy of HCl in the range 6 to 140 kJ mol^{-1}. This implies that proton exchanged molecules have lost memory of the initial HCl trajectory. Moreover, the independence of the proton exchanged fraction of the impinging molecules on their initial momentum also excludes the possibility of an entry of HCl by ballistic penetration through the interface, since this process should be a function of the impact energies. In addition, the desorption of DCl molecules from the liquid with velocities having a Maxwell–Boltzmann distribution proves that there is no H → D exchange channel that bypasses the thermal equilibration step. These observations support the assumption of a two-step process, in which HCl first thermally equilibrates in the interfacial region and then reacts, as proposed by Nathanson and co-workers.[19,20,33]

The experimental results allow the exchange process to be separated into two successive steps, for which the exchange probability, P_{exch}, is a product of the trapping probability, P_{trap}, and the fraction of trapped molecules that undergo exchange, f_{exch}, as expressed by eqn (7), *viz.*

$$P_{exch}(E_{inc},\theta_{inc},T_{liq},\text{ wt\%}) = P_{trap}(E_{inc},\theta_{inc},T_{liq},\text{ wt\%})\, f_{exch}(T_{liq},\text{ wt\%}) \quad (7)$$

Within this framework the exchange rate depends on the trapping probability, the temperature and the composition of the liquid surface. With the assumption that all molecules in thermal equilibrium with the liquid are momentarily trapped at the surface before desorbing or reacting, the proton exchange fraction, as given by the ratio of the integrated areas of thermally desorbing HCl and DCl molecules, $f_{exch} \equiv TD_{DCl}/(TD_{DCl} + TD_{HCl})$, can be expressed in terms of a competition between the proton exchange reaction and the desorption of thermalized HCl molecules within the liquid. Since the ratio of DCl to HCl thermal desorption intensities equals the ratio of rates for H → D reaction and desorption of thermalized HCl molecules, the exchange fraction to be expressed as

$$f_{exch} \equiv TD_{DCl}/(TD_{DCl} + TD_{HCl}) = k_{exch}/(k_{exch} + k_{des}) \quad (8)$$

where k_{des} is the rate constant for HCl desorption, averaged over all adsorption sites, and k_{exch} is the rate constant for H → D exchange, encompassing both interfacial and solution phase solvation and reaction.[20] The total exchange probability then equals the product of the trapping probability and f_{exch}, *viz.*

$$P_{exch} = P_{trap}f_{exch} = P_{trap}k_{exch}/(k_{exch} + k_{des}) \quad (9)$$

Information on the residence time of dissolved molecules can be obtained from pulsed experiments. Using this technique it has been shown[20,34] that HCl molecules desorb on a timescale of <2 μs and do not appear to enter the liquid. On the other hand, all molecules which undergo proton exchange spend at least some time in solution.[20,34] These observations imply that k_{sol} and k_{exch} should be equal and hence

$$P_{exch} = P_{trap}k_{sol}/(k_{sol} + k_{des}) \quad (10)$$

Eqn (10) is equivalent to the expression for the mass-accommodation coefficient, α, *viz.*

$$\alpha = Sk_{sol}/(k_{sol} + k_{des}) \quad (11)$$

In this expression it is assumed that the probability for trapping of molecules (P_{trap}) is equal to the sticking coefficient S.[34] This is supported by the fact that the energy of interaction between gas phase HCl and surface molecules ($\sim$28 kJ mol^{-1}) is larger than the thermal energy after desorption.

The advantage of time and energy resolved molecular beam experiments is the direct determination of the sticking

coefficient, S, and hence the possibility to distinguish between k_{sol} and k_{des} as well as to determine the mass accommodation coefficient directly. Our experiments performed at low initial energies (5/2 RT) prove that the probability for impinging HCl molecules to reach thermal equilibrium on a sulfuric acid–water surface is close to unity.

4.2 Mass accommodation for different acid concentrations

As discussed in the previous section, the fractional energy release of colliding HCl molecules onto the fluid interface is nearly independent of the acid concentration in the range 54–70 wt% and at 213 K. Nevertheless, the binding properties between HCl and interfacial D_2O and D_2SO_4 which allow thermalized molecules to be transported into the liquid phase and to undergo proton exchange, decrease substantially over this concentration range. The data displayed in Fig. 6 indicate a significant change in the ability to enter the liquid phase at concentrations between 50 and 70 wt%. At high acid concentrations (>70 wt%), the probability for HCl to be transported into the liquid phase is only 0.3. Therefore, about 70% of the thermalized HCl molecules desorb from the surface after dissipating their collisional energy and hence escape before solvation and dissociation. The fraction of molecules that reside on the surface long enough for D_2O and D_2SO_4 to reorganize and be available for solvation increases with increasing water content and reaches a value of 0.7 at 54 wt% acidity.

Comparable observations were also made in uptake measurements in which a marked decrease in the potential to remove HCl from the gas phase was observed with increasing acidity of the H_2SO_4–H_2O solution.[16,18,31] As mentioned in the introduction, the gas phase concentration change of HCl in contact with sulfuric acid–water solutions has been investigated by several groups using different experimental techniques.[8,14–23]

It is interesting to note that uptake coefficients or γ values, as reported by Watson *et al.*,[17] Robinson *et al.*,[18] Hanson and Lovejoy[16] and Tolbert *et al.*[15] using different experimental techniques, equally show a substantial decrease over the concentration range 50 to 80 wt%. This demonstrates that the uptake coeficient may well be limited by surface accommodation.

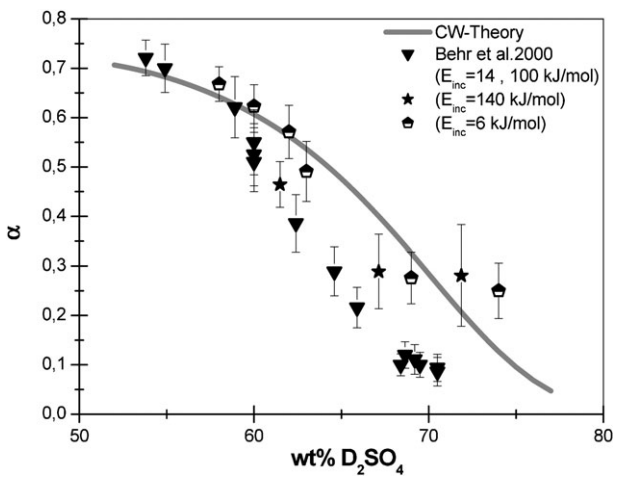

Fig. 6 Measured α-values *versus* acidity (in wt%) in comparison with literature data for the uptake of HCl on sulfuric acid solutions. The solid curve was calculated using the capillary wave theory of mass accommodation (see text).

Despite this consistency, the rate limiting step which is responsible for the decrease in the uptake of HCl as a function of the acidity is still discussed quite controversially.

For example, the results from droplet train experiments of Robinson *et al.*[18] in which the time dependent uptake, $\gamma(t)$, of HCl in contact with H_2SO_4 solutions at concentrations between 39 and 69 wt% was measured, led to the conclusion that the observed decrease in uptake with increasing acidity is due to a change in the solubility as expressed by the product of $(H^*D_l)^{1/2}$, rather than by a change in the mass accommodation coefficient. The authors estimated α to be always near unity at 230 K, independent of acidity. In contrast, the measurements presented in this work indicate that the observed change in the uptake of HCl as a function of acidity at 213 K is caused by a change of the probability of thermalized molecules to be transported through the phase boundary, as evidenced by a change in mass accommodation.

According to Davidovits *et al.*[5] the temperature dependence of mass accommodation is governed by the thermodynamic equilibrium between the species in the gas phase and the critical cluster in the solvated phase with the Gibbs energy being $\Delta G_{obs} = \Delta H_{obs} - T\Delta S_{obs}$. The functional form of ΔG_{obs} depends on the theoretical formulation of the uptake process and hence ΔG_{obs} can serve as a bridge between theory and experiment. Robinson *et al.*[18] reported a decrease in the mass accommodation coefficient with increasing temperature. The thermodynamic parameters were quantitatively described by the critical cluster model of mass accommodation[5,35] in which dynamic interactions of surface molecules are treated in terms of nucleation theory. A more detailed description of the assumptions and approximations made in this model has been provided by Nathanson *et al.*[9] The predicted number of three water molecules which form a critical cluster size is in agreement with quantum chemical approaches in which the minimum number of water molecules required for dissociation of HCl has been calculated.[36–38]

The surface kinetics associated with mass accommodation and its dependence on the dynamics at the fluid interface can be qualitatively discussed using the capillary wave (CW) model.[39] In this model the cluster-size parameter of Davidovits *et al.*[5] is replaced by an effective coordination number for a solute molecule that is in the process of penetrating into and below the liquid surface.[39] Penetration is effected through the random motions of the liquid surface. The progress of uptake is then characterized by the increase in coordination number, defined as the number of solvent molecules surrounding and in contact with the solute molecule. Upon complete solvation it reaches a maximum value which is characteristic for the bulk solution.

On a molecular scale surface motion can be regarded as a superposition of normal capillary waves forming local modes which are typically characterised by a fast rise time, $\tau_1 = \rho/2k^2\eta$, and slow decay time, $\tau_2 = 2\eta/k\phi$. The parameters ρ, η, and ϕ are, respectively, the density, the coefficient of viscosity, and the surface tension of the liquid; the value

k represents the wave vector $2\pi/\lambda$. In the picture of mass accommodation the solute molecule is assumed to become part of a collapsing local mode as it gets incorporated into the bulk liquid. In order to estimate the time scale for mass accommodation of HCl on sulfuric acid–water solutions we assume that the width of the local mode is about 10^{-9} m $\sim \lambda/2$ (3 molecular diameters) and hence the wave vector k equals 3×10^9 m. With this assumption the time period of the collapsing local mode is $\tau_2 = 4.5 \times 10^{-9}$ s at 213 K and for 54 wt% acidity. This period increases by more than an order of magnitude as the acidity and hence the viscosity increase.[40] In contrast, the change in surface tension[41] has only a minor effect. In the concentration range between 54 and 76 wt% the corresponding rate coefficient k_{sol} decreases from 2.2×10^8 s^{-1} to 7.4×10^6 s^{-1} at 213 K. The solid curve in Fig. 6 represents the calculated mass accommodation coefficient (k_{sol}/k_{des}) in dependence of the acidity of the liquid phase. At 64 wt% where the probabilities of thermally equilibrated molecules to either enter the liquid phase or to desorb with thermal speed are equal, we assume that $k_{des} = k_{sol} \sim 1 \times 10^8$ s^{-1}.

It needs to be mentioned that the oscillation period of the fastest waves is about 4.5×10^{-9} s in a sulfuric acid–water mixture at 213 K and for 54 wt% acidity. This is quite long in comparison with the duration of a collision with the surface for a gas molecule of kinetic energy larger than the average thermal energy. In the molecular beam experiments reported here the liquid surface will therefore usually appear as a frozen landscape and the transfer of collision energy into the capillary-wave spectrum will be very inefficient. However, this is not necessarily true for low-energy collisions.

The estimated desorption rate constant k_{des} can be compared with available literature information. We assume that hydrogen bonding between HCl and surface OD and SO groups should provide the strongest bonds. In this case the most pertinent information for hydrogen bonding of HCl to the surface of sulfuric acid comes from studies of HCl adsorption at the surface of ice and of solid $HCl{\cdot}6H_2O$.[42–45] The adsorption energy and Arrhenius pre-exponential factor, respectively, of $E_{ads} = 28$ kJ mol^{-1} and $\nu_{des} = 2 \times 10^{14}$ s^{-1}, as measured by Isakson and Sitz,[42] predict a k_{des}-value for HCl of 2.7×10^7 s^{-1} at 213 K. In addition, we have no indication that this rate constant is significantly influenced by the composition of the liquid phase (*cf.* Behr *et al.*[34]).

4.3 Temperature dependence of mass accomodation

The observed increase of the mass accommodation coefficient, α, with increasing temperature is shown is Fig. 7. The results shown imply that the solvation rate is more strongly enhanced by the thermal motions of the surface molecules than the desorption rate. For a discussion of this observation we have to consider that both kinetic parameters, k_{des} and k_{sol}, are temperature dependent.

According to capillary wave theory the temperature dependence of k_{sol} is mainly given by the temperature dependence of the viscosity which decreases from 4450 cP to 195 cP in the temperature range 210–240 K.[40] The effect of the surface tension is comparatively weak.[41] The corresponding value of k_{sol} therefore increases from 2.5×10^7 s^{-1} at 213 K to 5.7×10^8 s^{-1} at 243 K. Regarding the temperature dependence of k_{des} we have used a desorption energy and pre-exponential factor of $E_{des} = 26$ kJ mol^{-1} and $\nu_{des} = 2 \times 10^{14}$ s^{-1}, respectively, very close to the values for HCl on ice and solid $HCl{\cdot}6H_2O$.[42] As can be seen from the comparison in Fig. 7 the agreement between experimental data and theoretical prediction is quite satisfactory. Although it must be noted that further adjustment of the input data might lead to further improvement we have no convincing justification to do so. Overall, however, the agreement between these results suggests that the binding of HCl on sulfuric acid–water solutions is dominated by hydrogen bonds between HCl molecules and dangling OH-groups and OD-groups, respectively.

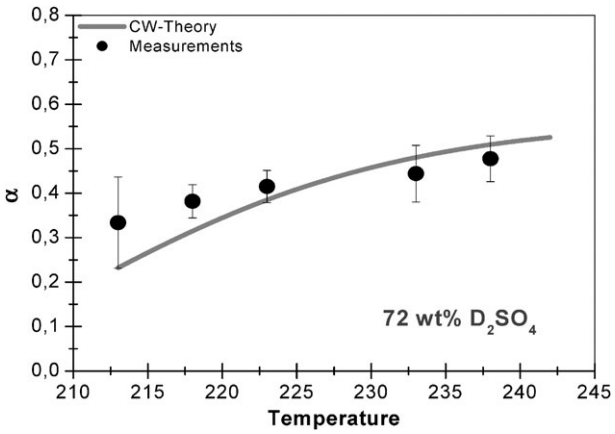

Fig. 7 Representation of mass accommodation coefficient as a function of temperature. The solid curve corresponds to the values of α as calculated on the basis of the temperature dependent rate coefficients k_{sol} and k_{des}.

As demonstrated above the application of capillary wave theory provides a method to describe and quantify mass accommodation and its temperature dependence. Nevertheless there are other frameworks with which our observations could be reconciled. One of these is the weakening of the OH bonds between solvent species at the surface with increasing thermal motions and therefore the increased availability to bind trapped HCl. In addition increased temperature may lead to increased diffusivity through the interface.

Note added in proof

After the present work has been submitted and whilst the reviewing process was in progress we became aware of a theoretical paper by D. Ardura and D. J. Donaldson entitled "Where does acid hydrolysis take place?" published in *Phys. Chem. Chem. Phys.* 2009, **11**, 857–863. The results from this work are essentially identical with the present findings, in particular what the location of dissociation of HCl molecules during phase transfer is concerned.

Acknowledgements

The authors gratefully acknowledge valuable comments made by the reviewers. One of them (U. S.) is grateful to the DEGUSSA Foundation for financial support during the course of this work.

References

1 B. J. Finlayson-Pitts and J. N. Pitts, *Atmospheric Chemistry*, Academic Press, New York, 2000.
2 R. Zellner, *Topics in Physical Chemistry*, ed. H. Baumgärtel, W. Grünbein and F. Hensel, guest editor R. Zellner, Steinkopff/ Springer, Darmstadt, 1999, vol. 6, pp. 181–247.
3 D. R. Hanson, *J. Phys. Chem. B*, 1997, **101**, 4998–5001.
4 S. Solomon, *Rev. Geophys.*, 1999, **37**, 275–316.
5 P. Davidovits, C. E. Kolb, L. R. Williams, J. T. Jayne and D. R. Worsnop, *Chem. Rev.*, 2006, **106**, 1323–1354.
6 P. V. Danckwerts, *Gas–Liquid Reactions*, McGraw-Hill, New York, 1970.
7 Q. Shi, P. Davidovits, J. T. Jayne, D. R. Worsnop and C. E. Kolb, *J. Phys. Chem. A*, 1999, **103**, 8812–8823.
8 D. R. Hanson and A. R. Ravishankara, *J. Phys. Chem.*, 1993, **97**, 12309–12319.
9 G. M. Nathanson, P. Davidovits, D. R. Worsnop and C. E. Kolb, *J. Phys. Chem.*, 1996, **100**, 13007–13020.
10 U. Pöschl, Y. Rudich and M. Ammann, *Atmos. Chem. Phys. Discuss.*, 2005, **5**, 2111–2191.
11 P. Behr, U. Scharfenort and R. Zellner, *Phys. Chem. Chem. Phys.*, DOI: 10.1039/b812751c.
12 P. V. Danckwerts, *Trans. Faraday Soc.*, 1951.
13 P. G. T. Fogg, in *Chemicals in the Atmosphere Solubility: Sources, and Reactivity*, ed. P. G. T. Fogg and J. M. Sangster, John Wiley & Sons, London, U.K., 2003.
14 L. R. Williams and D. M. Golden, *Geophys. Res. Lett.*, 1993, **20**, 2227–2230.
15 M. A. Tolbert, M. J. Rossi and D. M. Golden, *Geophys. Res. Lett.*, 1988, **15**, 847–850.
16 D. R. Hanson and E. R. Lovejoy, *J. Phys. Chem.*, 1996, **100**, 6397–6405.
17 L. Watson, J. van Doren, P. Davidovits, D. Worsnop, M. Zahniser and C. Kolb, *J. Geophys. Res., [Atmos.]*, 1990, **95**, 5631–5638.
18 G. N. Robinson, D. R. Worsnop, J. T. Jayne, C. E. Kolb, E. Swartz and P. Davidovits, *J. Geophys. Res., [Atmos.]*, 1998, **103**, 25371–25381.
19 P. Behr, J. R. Morris, M. D. Antman, B. R. Ringeisen, J. R. Splan and G. M. Nathanson, *Geophys. Res. Lett.*, 2001, **28**, 1961–1964.
20 J. R. Morris, P. Behr, M. D. Antman, B. R. Ringeisen, J. Splan and G. M. Nathanson, *J. Phys. Chem. A*, 2000, **104**, 6738–6751.
21 M. Schwell, H. Baumgärtel, I. Weidinger, B. Krämer, H. Vortisch, L. Wöste, T. Leisner and E. Rühl, *J. Phys. Chem. A*, 2000, **104**, 6726–6732.
22 C. Mund and R. Zellner, *ChemPhysChem*, 2003, **4**, 638–645.
23 C. Mund and R. Zellner, *J. Mol. Struct.*, 2003, **661–662**, 491–500.
24 S. P. Sander, M. J. Kurylo, V. L. Orkin, D. M. Golden, R. E. Huie, B. J. Finlayson-Pitts, C. E. Kolb, M. J. Molina, R. R. Friedl, A. R. Ravishankara and G. K. Moortgat, *Chemical Kinetics and Photochemical Data for Use in Atmospheric Studies*, JPL Publication, 2003, pp. 02–25.
25 Q. Shi, J. T. Jayne, C. E. Kolb, D. R. Worsnop and P. Davidovits, *J. Geophys. Res., [Atmos.]*, 2001, **106**, 24259–24274.
26 K. S. Carslaw, S. L. Clegg and P. Brimblecombe, *J. Phys. Chem.*, 1995, **99**, 11557–11574.
27 J. K. Klassen, Z. J. Hu and L. R. Williams, *J. Geophys. Res., [Atmos.]*, 1998, **103**, 16197–16202.
28 T. Peter, *Annu. Rev. Phys. Chem.*, 1997, **48**, 785.
29 K. S. Carslaw, M. Wirth, A. Tsias, B. P. Luo, A. Doőrnbrack, M. Leutbecher, H. Volkert, W. Renger, J. T. Bacmeister and T. Peter, *Nature*, 1998, **391**, 675.
30 *Advanced Series in Physical Chemistry 3*, ed. C. E. Kolb, D. R. Worsnop, M. S. Zahniser, P. Davidovits, L. F. Keyser, M.-T. Leu, M. J. Molina, D. R. Hanson, A. R. Ravishankara, L. R. Williams, M. A. Tolbert and J. R. Barker, World Scientific, River Edge, NJ, 1995, p. 771.
31 J. M. Van Doren, L. R. Watson and P. Davidovits, *J. Phys. Chem.*, 1990, **94**, 3265–3269.
32 M. E. Saecker and G. M. Nathanson, *J. Chem. Phys.*, 1993, **99**, 7056–7074.
33 G. M. Nathanson, *Annu. Rev. Phys. Chem.*, 2004, **55**, 231–255.
34 P. Behr, K. Ataya and R. Zellner, in preparation.
35 D. R. Worsnop, M. S. Zahniser, C. E. Kolb, J. A. Gardner, L. R. Watson, J. M. van Doren, J. T. Jayne and P. Davidovits, *J. Phys. Chem.*, 1989, **93**, 1159–1172.
36 S. Re, Y. Osamura, Y. Suzuki and H. F. Schaefer III, *J. Chem. Phys.*, 1998, **109**, 973–977.
37 S. C. Xu, *J. Chem. Phys.*, 1999, **111**, 2242–2254.
38 M. Tachikawa, M. Kazuhide and Y. Osamura, *Mol. Phys.*, 1999, **96**, 1207–1215.
39 C. J. H. Knox and L. F. Phillips, *J. Phys. Chem. B*, 1998, **102**, 8469–8472.
40 L. R. Williams and F. S. Long, *J. Phys. Chem.*, 1995, **99**, 3748–3751.
41 C. E. L. Myhre, C. J. Nielsen and O. W. Saastad, *J. Chem. Eng. Data*, 1998, **43**, 617–622.
42 M. J. Isakson and G. O. Sitz, *J. Phys. Chem. A*, 1999, **103**, 2044–2049.
43 J. D. Graham and J. T. Roberts, *J. Phys. Chem.*, 1994, **98**, 5974–5983.
44 D. C. Clary and L. C. Wang, *J. Chem. Soc., Faraday Trans.*, 1997, **93**, 2763–2767.
45 B. J. Gertner and J. T. Hynes, *Science*, 1996, **271**, 1563–1566.